Published in "European Journal of Inorganic Chemistry
2015(34): 5628–5638, 2015"
which should be cited to refer to this work.

Towards Cardiolite-Inspired Carbon Monoxide Releasing Molecules – Reactivity of d^4, d^5 Rhenium and d^6 Manganese Carbonyl Complexes with Isocyanide Ligands

Emmanuel Kottelat,[a] Valentin Chabert,[a] Aurélien Crochet,[b][‡] Katharina M. Fromm,[a][‡] and Fabio Zobi*[a]

Keywords: Carbon monoxide / Rhenium / Manganese / Isocyanide ligands

Carbon monoxide releasing molecules (CORMs) are investigated widely in synthetic and medicinal chemistry owing to the potential therapeutic applications of the CO gas. Organometallic carbonyl complexes are best suited to play the role of CO carriers as they allow the exogenous release of CO under controlled conditions, and the toxicity of the gas can be overcome. With the long-term goal of developing CORMs with similar properties to those of the sesta-methoxyisobutylisonitrile (sesta-mibi) ^{99m}Tc complex (Cardiolite), we have studied the reactivity of isocyanide ligands towards 16- and 17-electron *cis*-$[Re(CO)_2Br_4]^{-/2-}$ species and the $[Mn(CO)_5Br]$ complex. Six different isocyanide ancillary ligands (CNR), including mibi, were selected for this study. Their reactions with *cis*-dicarbonyl Re^{III} and Re^{II} complexes were accompanied by two- and one-electron reduction of the metal center and resulted in the formation of stable *cis-mer*-$[Re(CO)_2(CNR)_3Br]$ species, whereas the same reactions with $[Mn(CO)_5Br]$ gave *fac*-$[Mn(CO)_3(CNR)_2Br]$ compounds. All of the complexes were fully characterized, and single-crystal X-ray diffraction structure determinations were performed for selected species. In addition, unique monocarbonyl complexes were obtained from the reactions of *cis*-$[Re(CO)_2Br_4]^-$ (**1**) with *tert*-butyl isocyanide and *cis*-$[Re(CO)_2Br_4]^{2-}$ (**2**) with mibi. The species, a heptacoordinate Re^{III} and a hexacoordinate Re^{II} complex, respectively, were also characterized structurally. The CO-releasing profiles, the cytotoxic effects against 3T3 fibroblast cells, and the antibacterial properties of the compounds were also investigated.

Introduction

Carbon monoxide (CO) is acknowledged as a fundamental neurotransmitter in humans and has recently received attention owing to its documented therapeutic effects. Like nitric oxide (NO) and hydrogen sulfide (H_2S), CO is produced endogenously in animals. These neurotransmitters are involved in several cellular, physiological, and pathological pathways, such as vasodilatation, endothelial injury, or inflammations.[1–10] The natural targets of CO are heme-containing proteins. Direct CO inhalation results in the formation of carboxyhemoglobin owing to the high affinity (ca. 230 times stronger than that of O_2) of the gas for the iron center of the protein.[11,12] The interaction of CO with hemoglobin constitutes a major barrier to the specific delivery of CO. To overcome this challenge, CO-releasing molecules (CORMs) are under investigation.[13–16]

In this respect, organometallic carbonyl complexes are best suited to play the role of CO carriers. Thus, the targeting of the molecules to local injuries can be achieved through the modification of the coordination sphere of the metal ion or by appending CORMs to biomolecules that accumulate in specific sites or to target-specific receptors. Romão and co-workers have proposed a conceptual model for the design of organometallic CORMs[17] in which different components should be considered for the synthesis of appropriate CORMs: the toxicity of the complex, the inner coordination sphere for the release of CO in response to a trigger, and the outer coordination sphere, obtained through the modification of ancillary ligands to modulate the pharmaceutical parameters (i.e., the biocompatibility, water solubility, and tissue targeting).

Rhenium and manganese ions are employed widely as metal centers for organometallic carbonyl complexes intended as CO carriers.[18–38] The Re-based CORMs tested to date have shown very low cytotoxicity towards different cell lines.[37,39] These complexes may be activated towards CO loss by the aquation of bound ions, and the rate of this substitution reaction can be modulated by the ancillary ligands.[37] On the other hand, Mn-based CORMs are activated by exposure to UV light and are known as photo-CORMs.[40–43]

With the above considerations in mind and with the long-term aim of developing Cardiolite-type CORMs, we report herein the reactivity of isocyanide ligands towards

[a] Department of Chemistry, University of Fribourg,
Chemin du Musée 9, 1700 Fribourg, Switzerland
E-mail: fabio.zobi@unifr.ch
http://www.chem.unifr.ch/en/research/zobi_group
[b] Fribourg Center for Nanomaterials (Frimat), University of Fribourg,
Chemin du musée 9, 1700 Fribourg, Switzerland
[‡] Members of the NCCR "Bioinspired Materials"
Supporting information for this article is available

16- and 17-electron *cis*-$[Re(CO)_2Br_4]^{-/2-}$ species and the $[Mn(CO)_5Br]$ complex. Cardiolite or sesta-methoxyisobutylisonitrile (sesta-mibi) ^{99m}Tc is a pharmaceutical agent used in imaging and accumulates specifically in the myocardium.[44,45] There are no reports of the reactivity of carbonyl complexes of Re in d^4 and d^5 electronic configurations with the above-mentioned ligands. Previous reports are all limited to Re^I d^6 species. On the other hand, carbonyl manganese chemistry is richer in this respect.[18–20,22–28] For the current study, we selected six different isocyanides (CNR), including mibi; the other ligands were: *tert*-butyl isocyanide (tbu), isopropyl isocyanide (ipp), cyclohexyl isocyanide (chx), (*S*)-(–)-α-methylbenzyl isocyanide (smb), and 1,1,3,3-tetramethylbutyl isocyanide (tmb). Their reactions with *cis*-dicarbonyl Re^{III} and Re^{II} precursors are accompanied by a two- or one-electron reduction of the metal center to yield stable *cis-mer*-$[Re(CO)_2(CNR)_3Br]$, whereas the same reactions with $[Mn(CO)_5Br]$ gave *fac*-$[Mn(CO)_3(CNR)_2Br]$ compounds. In addition, unique monocarbonyl species were obtained from the reactions of *cis*-$[Re(CO)_2Br_4]^-$ (**1**) with tbu and *cis*-$[Re(CO)_2Br_4]^{2-}$ (**2**) with mibi. All complexes were characterized fully [^1H NMR spectroscopy, cyclic voltammetry (CV), MS, and IR spectroscopy], and single-crystal X-ray diffraction structure determinations of selected compounds were performed. The CO-releasing properties, the antibacterial effects, and the cytotoxic effects of the compounds against fibroblast cells are also reported.

Results and Discussion

Reactivity of $[NEt_4][Re(CO)_2Br_4]$ and $[NEt_4]_2[Re(CO)_2Br_4]$ with CNR

Before our investigation, reactions involving isocyanides (CNR) and rhenium carbonyl species were described by the group of Ko[46] and restricted to Re^I d^6 complexes. By starting with $[Re(CO)_5Br]$ and following different synthetic strategies, the authors could access *fac*-$[Re(CO)_3(CNR)_2Br]$, *fac*-$[Re(CO)_3(CNR)_3]$, and *cis-mer*-$[Re(CO)_2(CNR)_3Br]$ species. In our case, regardless of the starting precursor, we found that the reactions of **1** (16-electron species) and **2** (17-electron species) with isocyanides gave stable 18-electron *cis-mer*-$[Re(CO)_2(CNR)_3Br]$ complexes [CNR = tbu (**3**), ipp (**4**), chx (**5**), smb (**6**), tmb (**7**), or mibi (**8**); see Scheme 1]. Furthermore, a heptacoordinate monocarbonyl species of formula $[ReCO(tbu)_3Br_3]$ (**3a**) was also isolated as a by-product of the reaction of **1** with tbu.

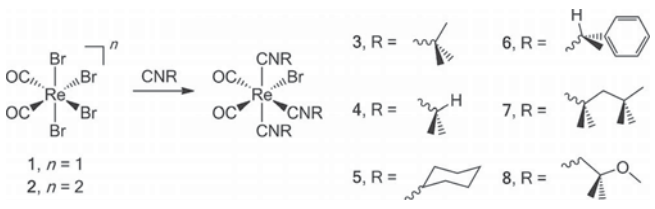

Scheme 1. General synthetic and numbering scheme of *cis-mer*-$[Re(CO)_2(CNR)_3Br]$ complexes derived from **1** and **2**.

To obtain insights into the mechanism of product formation, the substitution reactions of **1** and **2** were monitored by in situ liquid IR spectroscopy upon the slow addition of the ligand (0.5 equiv. every 5 min for 100 min). Representative spectra for the formation of **3**, **5**, **6**, and **8** are shown in Figure 1. With the exception of **3**, all reactions gave similar wavenumber patterns regardless of the starting precursor. The peaks of the starting compound in a dichloromethane (DCM) solution appear at $\tilde{\nu} \approx 2073$ and 2006 cm^{-1}. After the addition of 1–2 equiv. of the ligand, an intermediate formed with νCO stretching frequencies at $\tilde{\nu} \approx 2040$ and 1940 cm^{-1}. In this initial phase, the vibration of the free ligand could not be observed; therefore, a rapid reaction occurs with the *cis*-$[Re(CO)_2]^{3+/2+}$ core. Indeed, a new signal at $\tilde{\nu} \approx 2200$ cm^{-1} (νCN stretching) evidenced the binding of CNR to the rhenium center. After the further addition of the ligand, both the CO and CNR frequencies suffered a supplementary bathochromic shift to $\tilde{\nu} \approx$ 1960–1880 and 2200–2125 cm^{-1}, respectively. No further changes were ob-

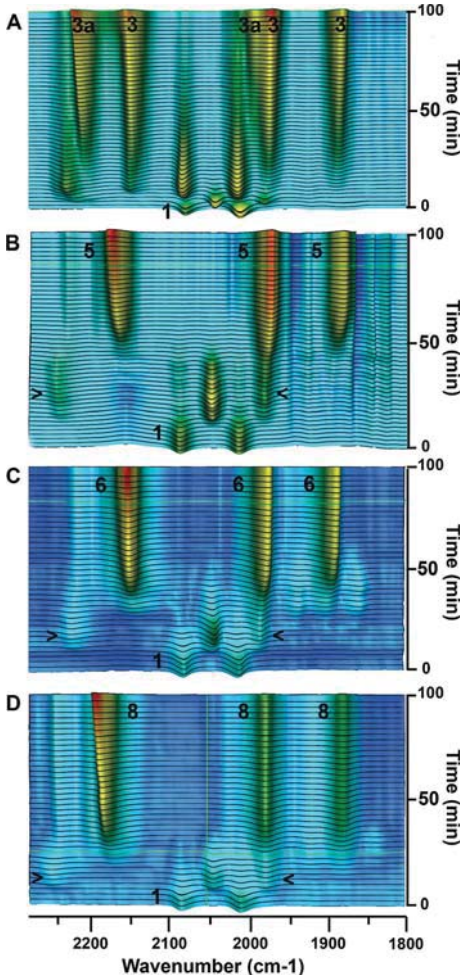

Figure 1. The evolution of the νCO and νCN bands in the in situ IR spectra of the reactions of **1** with (A) *tert*-butyl isocyanide, (B) cyclohexyl isocyanide, (C) (*S*)-(–)-α-methylbenzyl isocyanide, and (D) mibi. The numbers on the spectra indicate the peaks assigned to the complexes formed (see Scheme 1 and Table 1), whereas the peaks enclosed within the > < symbols refer to the intermediates formed. Reaction conditions: 25 °C in dry CH_2Cl_2.

served upon the addition of an excess of CNR. The final dicarbonyl species, identified as the *cis-mer*-$[Re(CO)_2(CNR)_3Br]$ products, showed more-intense vibrations than those of the starting material or the intermediates. Despite our efforts, the intermediates could not be isolated; however, a computational vibrational analysis of the substitution reactions at the DFT level of theory is provided below.

For tbu as the ligand, the formation of **3** was monitored by liquid IR spectroscopy, and a more complicated signal pattern was observed. Two intermediates were observed and two distinct final products formed. One of them ($\tilde{\nu}$ = 2137 cm^{-1}, νCN stretching; $\tilde{\nu}$ = 1973 and 1894 cm^{-1}, νCO vibrations) is the *cis-mer*-$[Re(CO)_2(CNR)_3Br]$ product **3**, whereas the second one was identified as a heptacoordinate Re^{III} monocarbonyl species ($\tilde{\nu}$ = 2196 cm^{-1}, νCN vibration; $\tilde{\nu}$ = 1991 cm^{-1}, νCO vibration) of formula $[Re(CO)(CNR)_3Br_3]$ (**3a**) after crystallographic analysis (vide infra, Figure 2).

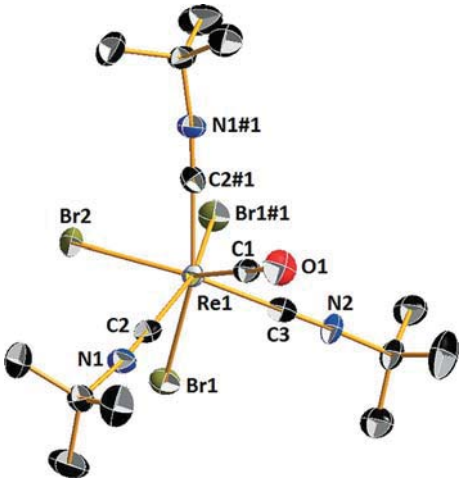

Figure 2. Molecular view of **3a**. Ellipsoids are drawn at 50% probability. Hydrogen atoms are omitted for clarity.

All of the Re-based complexes are air and thermally stable species with good solubility in common organic solvents. Overall, we attribute the formation of stable low-spin 18-electron species to the strong π-acidity of the CNR ligands. Complexes **3a**, **4**, and **8** were characterized structurally by X-ray crystallography (vide infra).

Reactivity of $[Mn(CO)_5Br]$ with CNR

Early studies by Treichel and co-workers showed that the reactions of $[Mn(CO)_5Br]$ with CNR give several different products, depending on the reaction conditions, and that the product distribution is dependent on the reaction time and on the ratio of reactants.[47] On the basis of this earlier work, a mixture of $[Mn(CO)_{5-n}(CNR)_nBr]$ (n = 2–4) could be expected. Later, Treichel also showed that the reactions of $[Mn(CO)_{5-n}(CNR)_nBr]$ complexes with excess CNR could produce *mer*- and *fac*-$[Mn(CO)_3(CNR)_3]^+$ and *cis-trans*-$[Mn(CO)_2(CNR)_4]^+$ complexes.[48] Under our experimental conditions, we found that the reactions of $[Mn(CO)_5Br]$ with 3–4 equiv. of CNR gave tricarbonyl Mn^I complexes of the general formula *fac*-$[Mn(CO)_3(CNR)_2Br]$ in all cases [CNR = tbu (**9**), ipp (**10**), chx (**11**), smb (**12**), tmb (**13**), or mibi (**14**); see Scheme 2]. After chromatographic purification, all of the compounds were isolated in high yields as crystalline powders. As expected for octahedral complexes bearing a *fac*-$[Mn(CO)_3]^+$ core, the isolated products were air and thermally stable but showed decomposition upon prolonged photoexposure. All of the species gave satisfactory elemental analyses and showed clean ^1H NMR spectra and positive-ion ESI mass spectra. Complexes **10**, **11**, and **14** were characterized structurally by X-ray crystallography.

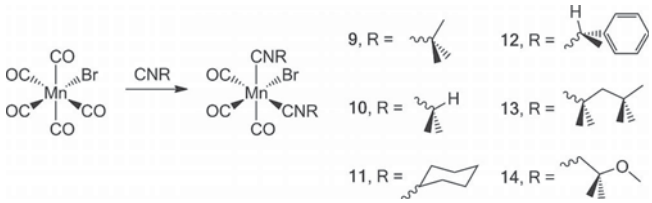

Scheme 2. General synthetic and numbering scheme of *fac*-$[Mn(CO)_3(CNR)_2Br]$ complexes derived from $[Mn(CO)_5Br]$.

Spectroscopic Characterization of Complexes and Electrochemical Analysis

The analytical data for **3**–**14** are summarized in Table 1. All of the complexes with general formula *cis-mer*-$[Re(CO)_2(CNR)_3Br]$ exhibit two strong νCO stretching vibrations in the $\tilde{\nu}$ = 1860–1900 and 1950–1970 cm^{-1} ranges and two νCN stretches (one strong and one weak) in the $\tilde{\nu}$ = 2120–2160 and 2190–2210 cm^{-1} ranges. The signals are consistent with the meridional arrangement of the ligands and the C_s symmetry of the octahedral complexes. Conversely, the complexes with the general formula *fac*-$[Mn(CO)_3(CNR)_2Br]$ are characterized by one strong νCN stretching peak in the $\tilde{\nu}$ = 2170–2211 cm^{-1} range and three νCO vibrations centered at $\tilde{\nu} \approx$ 2030, 1970, and 1920 cm^{-1}. The Re-based compounds (i.e., **3**–**8**) show strong absorptions in the blue regions of the UV/Vis spectrum with peaks centered at λ = 220 nm and a band with a lower molar extinction at λ =

Table 1. Analytical data of **3**–**14**.

	Solid-state IR [cm^{-1}][a]	λ_{max} [nm][b]	$E_{1/2}$ [V][c]
3	2189, 2121 (νCN), 1956, 1865 (νCO)	314	+1.16
4	2195, 2136 (νCN), 1967, 1898 (νCO)	318	+1.36
5	2201, 2128 (νCN), 1956, 1864 (νCO)	318	+1.22
6	2198, 2124 (νCN), 1959, 1880 (νCO)	314	+1.28
7	2198, 2123 (νCN), 1958, 1878 (νCO)	320	+1.18
8	2211, 2159 (νCN), 1967, 1889 (νCO)	314	+1.15
9	2176 (νCN), 2032, 1967, 1913 (νCO)	415	–
10	2180 (νCN), 2033, 1974, 1932 (νCO)	383	–
11	2181 (νCN), 2031, 1969, 1922 (νCO)	384	–
12	2176 (νCN), 2035, 1979, 1935 (νCO)	384	–
13	2171 (νCN), 2031, 1977, 1931 (νCO)	387	–
14	2211 (νCN), 2032, 1969, 1922 (νCO)	384	–

[a] On spring diamond. [b] In methanol. [c] Relative to Re^I to Re^{II} redox potential, versus saturated calomel electrode (SCE), in CH_3CN.

314–320 nm (Table 1). For the Mn-based complexes, the maximum absorbance was centered at λ = 250 nm, and a lower absorptivity band appeared between λ = 383 and 387 nm (Table 1). These features are consistent for **10**–**14**, whereas **9** shows a lower-energy band at λ = 415 nm. The latter bands are ascribed to the intraligand isocyanide $\pi \rightarrow \pi^*$ transition.[46] Complex **9** shows a lowest energy absorption from the $\pi \rightarrow \pi^*$ transition, which is due to a higher-energy highest occupied molecular orbital (HOMO) caused by the increased electron density on the tbu ligand as compared with those of the other isocyanides ligand.

X-ray Crystallography

The crystallographic details of **3a**, **4**, **8**, **10**, **11**, and **14** are summarized in Table 2, and selected bond lengths and angles are listed in Table 3. The molecular structures of the Re- and Mn-based complexes are given in Figures 2, 3, 4, 5, 6 and 7, respectively. As expected from the spectroscopic analyses, the CNR ligands assume *mer* conformations around the Re ions and *cis* conformations in the Mn compounds, whereas the CO ligands are observed in *cis* and *fac* arrangements, respectively. Complex **3a** was identified as a heptacoordinate d^4 Re species. Structurally characterized seven-coordinate 18-electron rhenium carbonyl complexes have been reported,[49–51] but, to the best of our knowledge, **3a** is the first example of a monocarbonyl Re^{III} species. In **3a**, the Re–CO bond length of 1.897(7) Å is not significantly different from the same bond lengths of the other Re species reported herein (see Table 3).

Isocyanide carbonyl rhenium complexes have been previously reported with the central metal ion bearing three carbonyl ligands.[46,52] To the best of our knowledge, **4** and **8** are the first examples of octahedral dicarbonyl Re species with isocyanide ligands. The bond lengths in **4** between the Re ion and C atoms from the CO ligands are 1.884(11) and 1.978(11) Å *trans* to Br and *trans* to isocyanide ligands, respectively, and exemplify the π-accepting/donor abilities of the two ligands. A similar effect can be seen in the structural parameters of **8** (more precisely species **8b** in Figure 4,

Table 2. Crystallographic data for **3a**, **4**, **8**, **10**, **11**, and **14**.

	3a	**4**	**8**	**10**	**11**	**14**
Formula	$C_{16}H_{27}Br_3N_3ORe$	$C_{14}H_{21}BrN_3O_2Re$	$C_{39}H_{66}Br_2ClN_6O_9Re_2$	$C_{11}H_{14}BrMnN_2O_3$	$C_{17}H_{22}BrMnN_2O_3$	$C_{15}H_{22}BrMnN_2O_5$
M_w	703.33	529.45	1330.65	357.09	437.21	445.19
T [K]	200(2)	200(2)	200(2)	200(2)	200(2)	200(2)
Lattice	monoclinic	monoclinic	triclinic	monoclinic	triclinic	triclinic
Space group	$P2_1/n$	$P2_1/c$	$P\bar{1}$	$P2_1/c$	$P\bar{1}$	$P\bar{1}$
Z	2	4	1	4	2	2
a [Å]	8.5672(7)	13.8904(14)	10.605(8)	6.120(2)	6.2131(8)	5.7667(6)
b [Å]	15.9603(11)	9.1443(9)	11.3827(10)	17.954(8)	10.6591(14)	11.2375(11)
c [Å]	8.6213(7)	15.0903(15)	11.3452(9)	14.642(5)	15.317(2)	15.4435(15)
α [°]	90	90	95.096(7)	90	97.228(11)	89.783(8)
β [°]	98.474(6)	98.412(8)	96.793(6)	99.38(3)	99.344(11)	81.639(8)
γ [°]	90	90	106.686(6)	90	98.655(11)	85.560(8)
V [Å^3]	1165.96(16)	1896.1(3)	1291.74	1587.3 (10)	977.7 (2)	987.15 (17)
d_{calcd} [g/cm^3]	2.003	1.855	1.711	1.494	1.485	1.498
R_1, wR_2	0.0209, 0.0465	0.0536, 0.1270	0.0394, 0.0995	0.0425, 0.662	0.0384, 0.0859	0.1020, 0.2517

Table 3. Selected crystallographic bond lengths [Å] and angles [°] for **3a**, **4**, **8**, **10**, **11**, and **14**.

3a		**4**		**8a**	
Re1–C1	1.897(7)	Re1–C1	1.884(11)	Re1–C1	1.941(3)
Re1–C2	2.036(4)	Re1–C2	1.978(11)	Re1–C2	2.04(3)
Re1–C3	2.039(6)	Re1–C3	2.056(9)	Re1–C3	2.11(3)
Re1–Br1	2.61(4)	Re1–C4	2.099(9)	Re1–C4	2.052(3)
Re1–Br2	2.607(7)	Re1–C5	2.051(9)	Re1–Br1	2.512(3)
		Re1–Br1	2.660(9)	Re1–Cl1	2.453(7)
C1–Re1–C2	74.57(15)	C1–Re1–C2	89.5(4)	C1–Re1–C2	90.4(9)
C1–Re1–C3	74.0(2)	C1–Re1–Br1	177.4(3)	C1–Re1–C3	178.6(10)
C1–Re1–Br1	125.81(8)			Br1–Re1–Cl1	176.64(19)
8b		**10**		**11**	**14**
Re2–C100	1.91(3)	Mn1–C1	1.832(6)	1.826(6)	1.848(6)
Re2–C101	2.069(4)	Mn1–C2	1.817(7)	1.779(7)	1.805(7)
Re2–C102	2.062(3)	Mn1–C3	1.803(6)	1.815(6)	1.847(6)
Re2–C103	2.07(3)	Mn1–C4	1.951(6)	1.942(6)	1.949(6)
Re2–C104	2.087(9)	Mn1–C5	1.946(5)	1.953(5)	1.952(5)
Re2–Br2	2.623(9)	Mn1–Br1	2.528(11)	2.526(9)	2.53(11)
C100–Re2–C102	91.1(10)	C1–Mn1–C2	92.4(2)	92.4(2)	91.9(3)
C100–Re2–C103	178.9(12)	C1–Mn1–C5	174.4(2)	175.4(2)	177.4(2)
C101–Re2–Br2	177.9(8)	C2–Mn1–Br1	178.94(17)	178.56(16)	176.87(19)

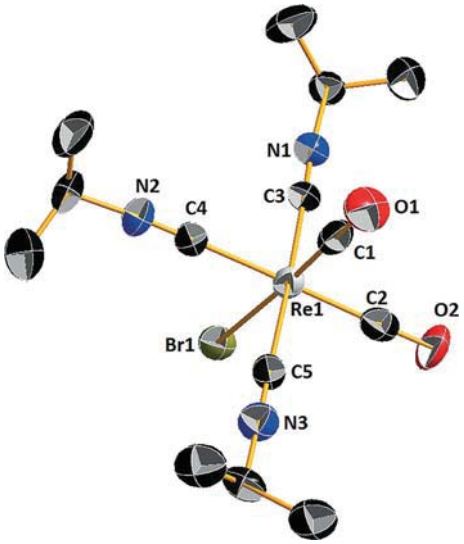

Figure 3. Molecular view of **4**. Ellipsoids are drawn at 50% probability. Hydrogen atoms are omitted for clarity.

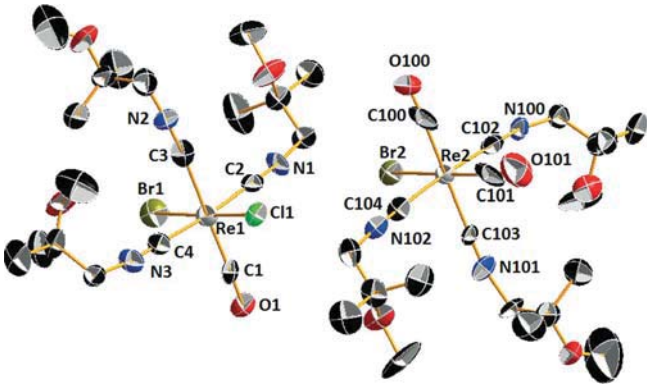

Figure 4. Molecular view **8a** (left) and **8b** (right). Ellipsoids are drawn at 30% probability. Hydrogen atoms are omitted for clarity.

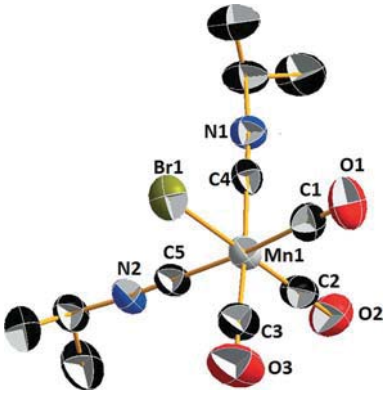

Figure 5. Molecular view of **10**. Ellipsoids are drawn at 50% probability. Hydrogen atoms are omitted for clarity.

vide infra). Interestingly, the inverted effect was observed elsewhere.[52] The solid-state structural analysis of crystals grown from solutions of **8** gave a unit cell with a 50:50 occupancy of two distinct molecules, namely, the expected $[Re(CO)_2(CNR)_3Br]$ complex (**8b** in Figure 4) and the

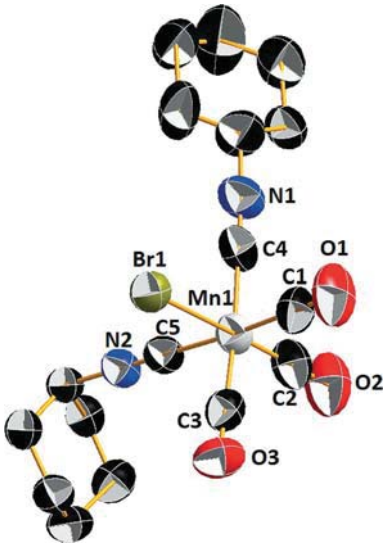

Figure 6. Molecular view of **11**. Ellipsoids are drawn at 50% probability. Hydrogen atoms are omitted for clarity.

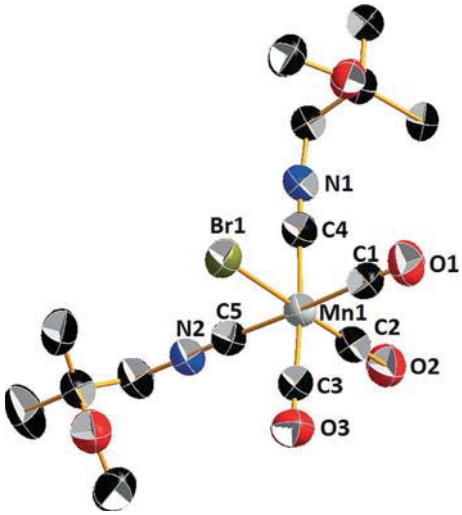

Figure 7. Molecular view of **14**. Ellipsoids are drawn at 50% probability. Hydrogen atoms are omitted for clarity.

unique monocarbonyl hexacoordinate Re^{II} $[ReCO(CNR)_3BrCl]$ species (**8a** in Figure 4). The analytical characterization of chromatographically purified and isolated powders of **8** did not show evidence of **8a**. Therefore, we assume that a CO ligand was lost during crystallization in CH_2Cl_2 and that the solvent acted as the chloride source. Examples of tricarbonyl manganese structures with two isocyanide ligands have also been reported.[53] Key angles and distances for structures **10**, **11**, and **14** are given in Table 3. No significant differences in terms of angles and bond lengths were found for these compounds compared to those described previously.

Computational Studies on CO Vibrational Energy by DFT

As outlined in a previous section, the reactions of **1** or **2** with CNR gave an intermediate after the addition of 1–

3 equiv. of the ligands before the formation of the final dicarbonyl product. As those intermediates were not isolated, we performed DFT calculations to gain insights into the reaction pathway to the *cis-mer*-$[Re(CO)_2(CNR)_3Br]$ species. For the calculations, the CNR ligands were reduced to $CNCH_3$ as the influence of substituents of the α-C atom was determined to be insignificant on the basis of spectroscopic characterization (Table 1). The molecular structures were first optimized without constraints (DFT level, B3LYP with LanL2DZ basis set), and then an IR frequency calculation was performed at the same level of theory. The gas-phase IR frequencies of **1** were first calculated and then normalized to the experimental values. The relative shifts of the νCO IR bands of all other species were then referenced to **1**.

All possible intermediates leading from **1** to the generic *cis-mer*-$[Re(CO)_2(CNR)_3Br]$ complex are depicted in Scheme 3. The intermediates in Scheme 3 are labeled to convey the binding arrangement of the incoming CNR, and the numbers indicate the oxidation state of the central atom. Thus, for example, it3 stands for an intermediate with one CNR ligand *trans* to a CO ligand in a Re^{3+} complex. Similarly, icc2 indicates an intermediate in which two CNR ligands are bound in a *cis* arrangement in a Re^{2+} complex. The relative positions of the calculated νCO IR bands were finally compared to the observed frequencies of the spectra recorded during the reaction and are plotted in Figure 8.

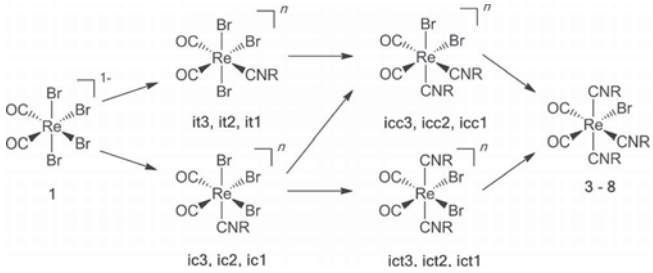

Scheme 3. Possible substitution pathways from starting compound **1** to the final general *cis-mer*-$[Re(CO)_2(CNR)_3Br]$ complex.

First, the calculations correctly predict the shift to lower wavenumbers of the νCO IR frequencies as a function of the reduced charge on the Re atom. The shifts are expected on the basis of an increased metal π-backbonding donation to the π* orbital of a CO ligand and a consequent reduction of the C–O bond order. In all cases, the νCO IR frequencies of related complexes follow the order Re^{3+} (green bars in Figure 8) > Re^{2+} (red bars) > Re^{+} (blue bars). As shown in Figure 8 (A and B), the observed CO bands cannot be assigned to Re^{3+} species. This indicates that the binding of a single CNR ligand is accompanied by a reduction of the metal center. On the basis of the theoretical frequencies, we tentatively assigned the intermediate product formed upon the addition of 1 equiv. of CNR to a mixture of ic2 and it2 in Scheme 3 (Figure 8, A and C).

The further addition of 2–3 equiv. of CNR did not produce experimentally clear shifts that were detectable with the in situ IR probe. As further substitution of Br^- ligands

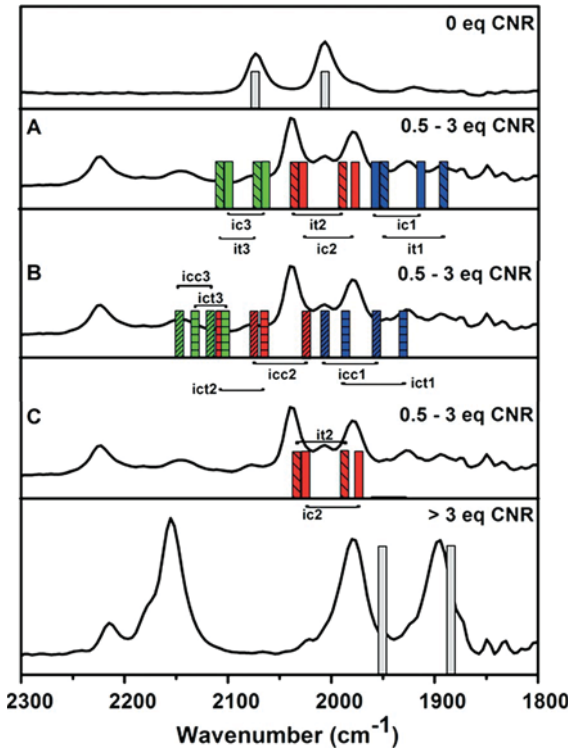

Figure 8. Comparison between the calculated (colored bars) and experimental (black spectra) values of the νCO frequencies for starting material **1**, potential intermediates, and the final product **3**–**8**. The labels of the intermediates are shown in Scheme 3.

occurs to form the final *cis-mer*-$[Re(CO)_2(CNR)_3Br]$ species, complexes bearing two CNR ligands were also calculated. The calculated frequencies of Re^{3+} and Re^{2+} complexes clearly move away from the experimental signals (green and red bars in Figure 8, B). This indicates that the binding of a second CNR ligand is accompanied by a second one-electron reduction of the metal center and that the bis-CNR intermediate is most likely a d^6 Re species. Indeed, the calculated frequencies of the Re^+ species move closer to the experimentally observed signals. This is particularly so for the calculated frequencies for icc1 (Scheme 3, Figure 8, B). Our findings agree with the work of Coe and Glenwright and, thus, owing to a slightly stronger *trans* effect of CO over CNR in rhenium complexes, we tentatively assign the second substitution product to icc1.[54] Overall, our theoretical analysis seems to point to the conclusion that the persistent intermediate observed in the reaction of **1** with 0.5–3 equiv. of CNR is a mixture of a mono-CNR d^5 Re complex and possibly the bis-CNR d^6 Re icc1 species.

CO-Releasing Properties

The CO-releasing properties of **3**–**14** were evaluated through the well-known myoglobin (Mb) assay.[37] Given the stability of closed-shell 18-electron rhenium carbonyl complexes, species **3**–**8** did not release carbon monoxide. The broad Q band corresponding to deoxy-Mb centered at $\lambda \approx 561$ nm remained unchanged in the presence of 1 equiv.

of **3**–**8** over a 2 h monitoring period. Somewhat to our surprise, the same result was obtained for **3a** (heptacoordinate d^4 Re complex) in the same assay. Compounds **9**–**14** were similarly tested through the Mb assay. The *fac*-$[Mn(CO)_3]^+$ species belong to a class of photoactive CORMs, and their CO-releasing properties were studied by eliciting CO liberation with 350 nm wavelength radiation. All Mn-based species were able to transfer carbon monoxide to Mb. Typical spectral changes of solutions of Mb in the presence of **8** and **14** are shown in Figure 9. The time required to reach CO saturation of Mb was also determined for the Mn species and is also shown in Figure 9. We found that the CO saturation of Mb was slowest for **9** and **14** (ca. twofold increase over the other species). Finally, experiments performed with substoichiometric amounts of **9**–**14** indicated that on average (2 ± 0.33) equiv. of CO are released by the complexes (data not shown).

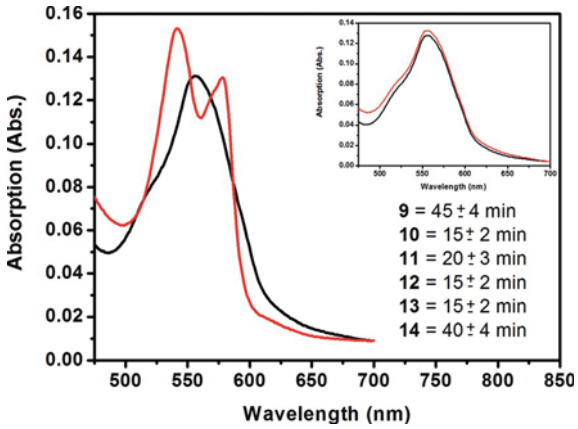

Figure 9. Typical spectral changes of solutions of Mb in the presence of rhenium (inset for **8**) and manganese carbonyl CNR complexes (**14**, 350 nm irradiation). The values below the inset refer to the time required for each Mn-based CORM to induce complete CO saturation of Mb. Black curve: initial spectrum, red curve: final spectrum. The data are expressed as the mean ± standard error of the mean (SEM) for three independent experiments.

Cell Proliferation Assay and Antibacterial Effects of 3–14

To assess the toxicity of our complexes, **3**–**14** were studied in a 3T3 fibroblast proliferation assay, and their antibacterial properties were tested against *Escherichia coli* bacteria. The biological results are summarized in Table 4,

Table 4. 3T3 fibroblast percentage cell viability and antibacterial effects of **3**–**14**.

	3T3 CP[a] [%]	MIC[b] [mg/mL]	Compound	3T3 CP [a] [%]	MIC[b] [mg/mL]
3	0	> 1	**9** (**9** + *hν*)[c]	7.9 (7.2)	> 1 (> 1)
4	24.5	> 1	**10** (**10** + *hν*)	75.9 (92.7)	> 1 (> 1)
5	0	> 1	**11** (**11** + *hν*)	3.3 (0.4)	> 1 (> 1)
6	7.7	> 1	**12** (**12** + *hν*)	3.0 (2.7)	0.13 (0.26)
7	0	> 1	**13** (**13** + *hν*)	0 (0)	> 1 (> 1)
8	88.8	> 1	**14** (**14** + *hν*)	60.6 (81.1)	> 1 (> 1)

[a] CP: cell proliferation after 72 h, 20 μM of compound. [b] MIC: minimum inhibitory concentration. [c] Compound number (compound number + *hν*): in the dark and (exposed to visible light for 30 min before inoculation).

and the effects of **3**–**8** and **9**–**14** on 3T3 fibroblast viability are shown in Figures 10 and 11, respectively. With the exception of species **8** bearing the mibi ligands, all of the Re-based complexes were toxic towards 3T3 fibroblast. Similar results were obtained for the Mn-based complexes. In this case, two sets of experiments were performed, whereby **9**–**14** were tested in the absence of light or irradiated before inoculation (Figure 11). Like the *cis-mer*-$[Re(CO)_2(CNR)_3Br]$ species, the Mn complexes showed a pronounced toxic

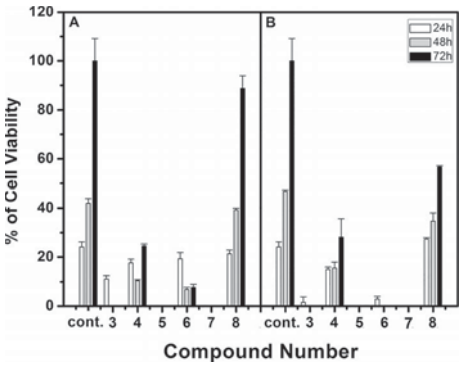

Figure 10. Effect on 3T3 fibroblast proliferation for **3**–**8** after 1 (white bars), 2 (grey bars), and 3 d (black bars): (A) 20 μM of compound; (B) 100 μM of compound.

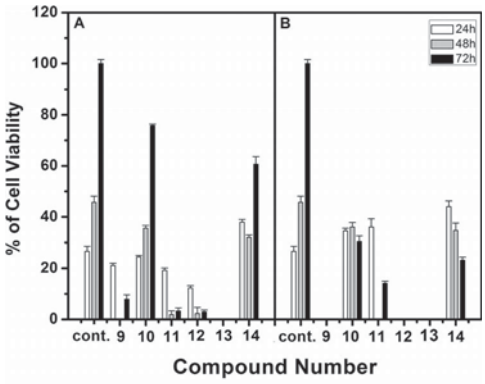

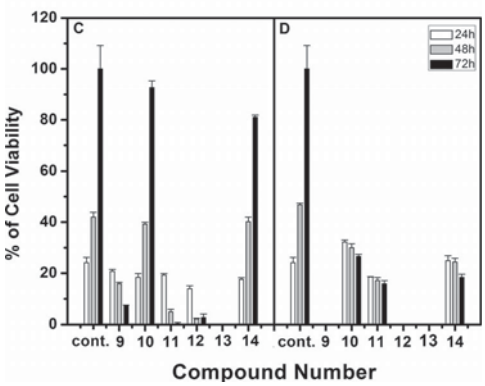

Figure 11. Effect on 3T3 mice fibroblast proliferation for **9**–**14** after 1 (white bars), 2 (grey bars), and 3 d (black bars): (A) 20 μM of compound in the dark before and after inoculation; (B) 100 μM of compound in the dark before and after inoculation; (C) 20 μM of compound exposed to visible light before and after inoculation; (D) 100 μM of compound exposed to visible light for 30 min before inoculation.

effect when incubated at 100 μM whether inoculated in the dark or previously exposed to light (Table 4). Conversely, when administered at 20 μM concentration and exposed to light, species **10** and **14** only slightly reduced cell proliferation; therefore, the relative inhibition of cell growth was mitigated by the induction of CO release before inoculation.

The cytotoxicity of the compounds prompted us to study the antibacterial effects of the molecules. Ruthenium and manganese CORMs have antimicrobial effects, although the cellular pathways are still poorly understood.[55–57] For this study, *E. coli* was selected, and species **9**–**14** were tested in the dark or after light activation. Our antibiograms revealed that none of the complexes (whether bearing Re or Mn) showed antibacterial properties with the exception of **12**. Species **12** showed minimum inhibitory concentrations (MICs) of 128 μg/mL if administered in the dark and 256 μg/mL if light-activated. Again, as observed in the cell proliferation assays, CO release seems to mitigate the toxic effects of the molecules. Although the MIC value for **12** is high with respect to the standard,[58,59] **12** could be used as a lead structure for further developments.

Conclusions

To develop Cardiolite CORM analogues, we have studied the reactivity of 16-, 17-, and 18-electron rhenium and manganese carbonyl species with isocyanide ligands. The reactions of CNR with *cis*-$[Re(CO)_2Br_4]^{-/2-}$ complexes are accompanied by two- and one-electron reductions of the metal center and result in the formation of *cis*-*mer*-$[Re(CO)_2(CNR)_3Br]$ 18-electron species, whereas the same reactions with $[Mn(CO)_5Br]$ gave *fac*-$[Mn(CO)_3(CNR)_2Br]$ compounds. The resulting Re complexes were stable and unable to release carbon monoxide. Conversely, the Mn species behaved as photoCORMs with light activation for CO release in the UV region of the electromagnetic spectrum. With the exception of compounds bearing the methoxyisobutylisonitrile (mibi) ligand, all molecules were toxic in a 3T3 fibroblast proliferation assay. None of the reported species showed high antibacterial effects. Persistent intermediates were observed in the reactions of **1** or **2** with CNR before the formation of the final dicarbonyl products. On the basis of a combined experimental and theoretical analysis, these intermediates were assigned to a mixture of a mono-CNR d^5 Re complexes and a bis-CNR d^6 Re species. The former might prove to be useful CORMs. Thus, further studies will be aimed at their isolation and characterization.

Experimental Section

Materials: Chemicals and solvents were purchased from standard sources. Real-time IR spectroscopy analyses were performed with a Mettler–Toledo react-IR 15 instrument. The UV/Vis spectra were recorded with a Perkin–Elmer Lambda 40 spectrometer. Solid-state IR spectra were recorded with a Bruker Tensor 27 instrument. The mass spectra were recorded with a Bruker esquire HCT spectrometer with methanol as solvent. The crystallographic data of single crystals were collected with Mo-K_α radiation (λ = 0.71073 Å), except for those of **14** which were measured with Cu-K_α radiation (λ = 1.54186 Å). All measurements were performed at 200 K with Stoe IPDS-II or IPDS-II T diffractometers equipped with Oxford Cryosystem open-flow cryostats.[60] The crystals were mounted on loops, and all geometric and intensity data were taken from these crystals. The absorption corrections were partially integrated in the data reduction procedure.[61] The structures were solved and refined by full-matrix least-squares techniques on F^2 with the SHELX-2014 package.[62] All atoms (except hydrogen atoms) were refined anisotropically. Hydrogen atoms were introduced as fixed contributors if a residual electronic density was observed near their expected positions.

CCDC-1402025 (for **3a**), -1402026 (for **4**), -1402027 (for **8**), -1402028 (for **10**), -1402029 (for **11**), and -1402030 (for **14**) contain the supplementary crystallographic data for this paper. These data can be obtained free of charge from The Cambridge Crystallographic Data Centre via www.ccdc.cam.ac.uk/data_request/cif.

Cyclic voltammetry was performed with the Echem software and a Princeton Applied Research 263 A instrument. For these measurements, 5 mM solutions of the organometallic species were prepared in 0.5 M tetrabutylammonium hexafluorophosphate as the electrolyte. The $[NEt_4][Re(CO)_2Br_4]$ (**1**) and $[NEt_4]_2[Re(CO)_2Br_4]$ (**2**) complexes were prepared according to a reported procedure[36] in yields of 46 (2.8 g, 6.91 mmol) and 60% (280 mg, 0.69 mmol), respectively.

DFT Calculations: Geometry optimizations and frequency calculations for all molecules were performed at the density functional level of theory with the Gaussian03 program package[63] with the hybrid B3LYP functional[64] in conjunction with the LanL2DZ basis set.[65–67] Pure basis functions (5d, 7f) were used in all calculations. The geometries were optimized fully without symmetry restrictions. The nature of the stationary points was checked by computing vibrational frequencies to verify true minima. The infrared spectra were calculated after geometry optimization in the gas phase (i.e., no solvation was considered).

Mibi Ligand: *Step 1:* $ZnCl_2$ (40 g, 293.8 mmol) was dissolved in dry methanol (27 mL). Then, 2-hydroxyisobutyronitrile (25 g, 293.8 mmol) was added under argon, and the solution was stirred at 60 °C overnight. At the end of the reaction, the obtained yellow solution was poured into an ice/water mixture (100 mL), extracted with diethyl ether (3 × 100 mL), and dried with $MgSO_4$, and the solvent was removed to afford 2-methoxyisobutyronitrile as a yellow liquid (yield 11.97 g, 120.5 mmol, 41%). *Step 2:* 2-Methoxyisobutyronitrile in diethyl ether (11.97 g, 120.5 mmol) was added dropwise to a solution of $LiAlH_4$ (5.50 g, 145 mmol) was in dry diethyl ether (300 mL) under argon. The solution was stirred at reflux overnight. At the end of the reaction, H_2O (80 mL) was added dropwise. The grey suspension was filtered, the solid was washed with diethyl ether, and the aqueous phase was then extracted with diethyl ether. The organic phases were dried with $MgSO_4$, and the solvent was removed to give 2-methoxyisobutylamine as a grey liquid (yield 3.77 g, 36.6 mmol, 30%). *Step 3*: Then, ethyl formate (2.9 mL, 36.6 mmol) was added dropwise to a solution of 2-methoxyisobutylamine (3.77 g, 36.6 mmol) in *p*-toluenesulfonic acid (0.017 g), and the mixture was stirred at reflux for 16 h. Then, the solvent was removed under high vacuum, and *N*-formyl-2-methoxyisobutylamine was obtained as am orange liquid (yield 3.2 g, 24.4 mmol, 67%). *Step 4: N*-Formyl-2-methoxyisobutylamine (3.2 g, 24.4 mmol) and trimethylamine (5.01 g, 49.5 mmol) were dissolved in CH_2Cl_2 (DCM, 36 mL). The mixture was cooled to –40 °C with an acetone/liquid nitrogen mixture. Then, diphosgene (1.46 mL) in dry DCM (18 mL) was added drop-

wise to the reaction mixture. The temperature of the mixture was increased to 0 °C, and the mixture was stirred at 0 °C for 1 h and then for 30 min at reflux. At the end of the reaction, H_2O (20 mL) was added, and the organic phase was washed with saturated sodium hydrogen carbonate and H_2O and dried with $MgSO_4$, and the solvent was removed to afford methoxyisobutylisonitrile (mibi) as a dark orange oil (yield 1.03 g, 9.16 mmol, 74%).

General Synthesis of *cis-mer*-[Re(CO)$_2$(CNR)$_3$Br] from 1 or 2: A solution of **1** or **2** (70 μmol) in DCM (2.5 mL) was placed in a small flask. Then, 0.5 equiv. of the isocyanide ligand (tbu, ipp, chx, smb, tmb, or mibi) was added every 5 min up to 10 equiv. of the ligand. At the end of the reaction, the solvent was removed, and purification was performed through silica column chromatography with DCM as the eluent. The purity of the collected compound was assessed by ^{1}H NMR spectroscopy, elemental analysis (EA), IR spectroscopy, and MS.

***cis-mer*-[Re(CO)$_2$(tbu)$_3$Br] (3):** Yield 30 mg, 52.5 μmol, 75%. IR: $\tilde{\nu}$ = 2189, 2121 (νCN stretching), 1955, 1865 (νCO stretching) cm^{-1}. ESI-MS (MeOH): *m*/*z* (%) = 492.1 (100) [M]$^+$. $C_{17}H_{27}BrN_3O_2Re$ (571.52): calcd. C 35.72, H 4.77, N 7.35; found C 35.21, H 4.67, N 7.12. ^{1}H NMR {360 MHz, [D$_6$]dimethyl sulfoxide ([D$_6$]DMSO)}: δ = 1.39 (s, 18 H, 6 × CH$_3$), 1.41 (s, 9 H, 3 × CH$_3$) ppm. ^{13}C NMR (500 MHz, [D$_6$]DMSO): δ = 29.5 (CH$_3$), 29.9 (CH$_3$), 30.3 (CH$_3$), 50.3, 139.2 (CNR), 188.5 (CO), 191.4 (CO) ppm.

***cis-mer*-[Re(CO)$_2$(ipp)$_3$Br] (4):** Yield 13 mg, 25.2 μmol, 36%. IR: $\tilde{\nu}$ = 2194, 2135 (νCN stretching), 1967, 1897 (νCO stretching) cm^{-1}. ESI-MS (MeOH): *m*/*z* (%) = 450.1 (100) [M]$^+$. $C_{14}H_{21}BrN_3O_2Re$ (529.44): calcd. C 31.76, H 4.01, N 7.93; found C 31.64, H 3.92, N 7.82. ^{1}H NMR (360 MHz, [D$_6$]DMSO): δ = 1.27 (t, *J* = 7.1 Hz, 18 H, 6 × CH$_3$), 4.19–4.23 (m, *J* = 14.2 Hz, 3 H, 3 × CH) ppm. ^{13}C NMR (500 MHz, [D$_6$]DMSO): δ = 23.0 (CH$_3$), 23.3 (CH$_3$), 48.0, 137.5 (CNR), 188.8 (CO), 192.0 (CO) ppm. Single crystals suitable for X-ray diffraction analysis were obtained by layering hexane on top of a DCM solution of the compound.

***cis-mer*-[Re(CO)$_2$(chx)$_3$Br] (5):** Yield 20 mg, 30.8 μmol, 44%. IR: $\tilde{\nu}$ = 2201, 2128 (νCN stretching), 1956, 1864 (νCO stretching) cm^{-1}. ESI-MS (MeOH): *m*/*z* (%) = 570.1 (100) [M]$^+$. $C_{23}H_{33}BrN_3O_2Re$ (649.64): calcd. C 42.52, H 5.13, N 6.47; found C 42.31, H 5.10, N 6.52. ^{1}H NMR (360 MHz, [D$_6$]DMSO): δ = 1.32–1.34 [m, 3 H, 3 × *p*-CH$_2$, axial (ax.)], 1.43–1.44 [m, 9 H, 6 × *m*-CH$_2$, ax., 3 × *p*-CH$_2$, equatorial (eq.)], 1.66–1.75 (m, 18 H, 6 × *m*-CH$_2$, eq., 6 × *o*-CH$_2$, ax., 6 × *o*-CH$_2$, eq.), 3.62–3.65 (t, *J* = 3.5 Hz, 3 H, 3 × CH) ppm. ^{13}C NMR (500 MHz, [D$_6$]DMSO): δ = 21.2, 21.4, 24.5, 24.6, 31.4, 31.8 (CH$_2$), 53.3 (CH) 138.8 (CN–R), 188.9 (CO), 190.0 (CO) ppm.

***cis-mer*-[Re(CO)$_2$(smb)$_3$Br] (6):** Yield 20 mg, 27.3 μmol, 39%. IR: $\tilde{\nu}$ = 2198, 2124 (νCN stretching), 1959, 1880 (νCO stretching) cm^{-1}. ESI-MS (MeOH): *m*/*z* (%) = 636.0 (100) [M]$^+$. $C_{29}H_{27}BrN_3O_2Re$ (715.66): calcd. C 48.67, H 3.81, N 5.87; found C 48.47, H 3.59, N 5.97. ^{1}H NMR (360 MHz, [D$_6$]DMSO): δ = 1.56–1.59 (d, *J* = 4.2 Hz, 6 H, 2 × CH$_3$), 1.61–1.63 (d, *J* = 6.8 Hz, 3 H, CH$_3$), 5.48–5.52 (m, *J* = 5.9 Hz, 3 H, 3 × CH), 7.33–7.56 (m, 15 H, 15 × benzyl-CH) ppm. ^{13}C NMR (500 MHz, [D$_6$]DMSO): δ = 24.7 (CH$_3$), 25.0 (CH$_3$), 25.1 (CH$_3$), 55.0 (CN-CH), 55.2 (CN-CH), 125.3 (benzyl-CH), 128.2 (benzyl-CH), 128.3 (benzyl-CH), 128.8 (benzyl-CH), 128.9 (benzyl-CH), 138.6 (CNR), 139.3 (CNR), 188.3 (CO), 191.4 (CO) ppm.

***cis-mer*-[Re(CO)$_2$(tmb)$_3$Br] (7):** Yield 25 mg, 35 μmol, 50%. IR: $\tilde{\nu}$ = 2198, 2123 (νCN stretching), 1958, 1878 (νCO stretching) cm^{-1}. ESI-MS (MeOH): *m*/*z* (%) = 660.3 (100) [M]$^+$. $C_{29}H_{51}BrN_3O_2Re$ (739.84): calcd. C 47.08, H 6.96, N 5.68; found C 47.28, H 7.11, N 5.77. ^{1}H NMR (360 MHz, [D$_6$]DMSO): δ = 1.18 (s, 18 H, 6 × C4-CH$_3$), 1.19 (s, 9 H, 3 × C4-CH$_3$), 1.51 (s, 12 H, 4 × C2-CH$_3$), 1.53 (s, 6 H, 2 × C2-CH$_3$), 1.60 (s, 4 H, 2 × CH$_2$), 1.62 (s, 2 H, CH$_2$) ppm. ^{13}C NMR (500 MHz, [D$_6$]DMSO): δ = 30.8 (CH$_3$), 30.9 (CH$_3$), 31.0 (CH$_3$), 31.17 (CH$_3$), 31.21 (CH$_3$), 50.3, 52.1, 52.8, 53.1, 55.1 (CH$_2$), 55.6 (CH$_2$), 160.3 (CNR), 188.6 (CO), 191.1 (CO) ppm.

***cis-mer*-[Re(CO)$_2$(mibi)$_3$Br] (8):** Yield 31 mg, 47.6 μmol, 68%. IR: $\tilde{\nu}$ = 2211, 2150 (νCN stretching), 1967, 1889 (νCO stretching) cm^{-1}. ESI-MS (MeOH): *m*/*z* (%) 582.2 (100) [M]$^+$. $C_{20}H_{33}BrN_3O_5Re$ (661.60): calcd. C 36.31, H 5.04, N 6.35; found C 36.43, H 4.98, N 6.27. ^{1}H NMR (360 MHz, [D$_6$]DMSO): δ = 1.22 (s, 18 H, 6 × C1-CH$_3$), 3.17 (s, 9 H, 3 × OCH$_3$), 3.91 (s, 4 H, 2 × CH$_2$), 3.93 (s, 2 H, 1 × CH$_2$) ppm. ^{13}C NMR (500 MHz, [D$_6$]DMSO): δ = 22.10 (CH$_3$), 22.14 (CH$_3$), 22.17 (CH$_3$), 49.4, 51.3 (CH$_2$), 51.5 (CH$_2$), 73.6 (OCH$_3$), 73.8 (OCH$_3$), 139.2 (CNR), 188.4 (CO), 191.5 (CO) ppm. Single crystals suitable for X-ray diffraction analysis were obtained by layering hexane on top of a methyl *tert*-butyl ether solution of the compound.

Isolation of [ReCO(tbu)$_3$Br$_3$] (3a): Compound **3a** was isolated as a byproduct from the reaction of **1** with tbu. First, a recrystallization of the reaction mixture was performed directly in DCM/hexane 1:2 to precipitate $(Et_4N)_2Br$. The solid was then collected by filtration, dried, and recrystallized again in DCM/hexane 1:2 to afford the pure complex **3a**. We noticed that this compound was removed (i.e., decomposed) during the chromatographic column performed to give the purified species **3**. Single crystals suitable for X-ray diffraction analysis were obtained by layering hexane on top of a DCM solution of the compound, yield 49 mg, 25.9 μmol, 37%.

General Synthesis of *fac-cis*-[Mn(CO)$_3$(CNR)$_2$Br]: [Mn(CO)$_5$Br] (55 mg, 200 μmol) was dissolved in acetone (2.5 mL). Then, the selected isocyanide ligand (700 μmol, 3.5 equiv.) was added, and the reaction mixture was stirred at reflux for 1 h. The solvent was removed, and the solid was purified by silica column chromatography with DCM/acetone 30:1 as the eluent. The solvent was removed, and the corresponding *fac-cis*-[Mn(CO)$_3$L$_2$Br] complex was obtained as a microcrystalline powder.

***fac*-[Mn(CO)$_3$(tbu)$_2$Br] (9):** Yield 30 mg, 78 μmol, 39%. IR: $\tilde{\nu}$ = 2176 (νCN stretching), 2032, 1967, 1913 (νCO stretching) cm^{-1}. ESI-MS (MeOH): *m*/*z* (%) = 360.1 (30) [M]$^+$. $C_{13}H_{18}BrMnN_2O_3$ (385.14): calcd. C 40.54, H 4.72, N 7.27; found C 40.78, H 4.68, N 7.19. ^{1}H NMR (360 MHz, [D$_6$]DMSO): δ = 1.41 (s, 18 H, 6 × CH$_3$) ppm. ^{13}C NMR (500 MHz, [D$_6$]DMSO): δ = 29.5 (CH$_3$), 31.3 (CH$_3$), 50.0, 150.8 (CNR), 214.4 (CO), 218.9 (CO) ppm.

***fac*-[Mn(CO)$_3$(ipp)$_2$Br] (10):** Yield 20 mg, 56 μmol, 28%. IR: $\tilde{\nu}$ = 2180 (νCN stretching), 2033, 1974, 1932 (νCO stretching) cm^{-1}. ESI-MS (MeOH): *m*/*z* (%) = 318.1 (20) [M]$^+$. $C_{11}H_{14}BrMnN_2O_3$ (357.09): calcd. C 37.00, H 3.96, N 7.85; found C 36.99, H 4.00, N 7.89. ^{1}H NMR (360 MHz, [D$_6$]DMSO): δ = 1.27–1.29 (d, *J* = 6.8 Hz, 12 H, 4 × CH$_3$), 4.19–4.23 (m, *J* = 7.6 Hz, 2 H, 2 × CH) ppm. ^{13}C NMR (500 MHz, [D$_6$]DMSO): δ = 22.8 (CH$_3$), 48.9, 152.8 (CNR), 214.3 (CO), 219.7 (CO) ppm. Single crystals suitable for X-ray diffraction analysis were obtained by layering hexane on top of a DCM solution of the compound.

***fac-cis*-[Mn(CO)$_3$(chx)$_2$Br] (11):** Yield 40 mg, 92 μmol, 46%. IR: $\tilde{\nu}$ = 2177 (νCN stretching), 2032, 1976, 1931 (νCO stretching) cm^{-1}. ESI-MS (MeOH): *m*/*z* (%) = 438.1 (15) [M]$^+$. $C_{17}H_{22}BrMnN_2O_3$ (437.21): calcd. C 46.70, H 5.08, N 6.41; found C 47.78, H 5.57, N 6.45. ^{1}H NMR (360 MHz, [D$_6$]DMSO): δ = 1.30–1.56 (m, 8 H, 4 × *o*-CH$_2$, eq.; 4 × *o*-CH$_2$, ax.) 1.63–1.91 (m, 12 H, 4 × *m*-CH$_2$, eq., 4 × *m*-CH$_2$, ax., 2 × *p*-CH$_2$, ax., 2 × *p*-CH$_2$, eq.), 4.31–4.37 (t, 2 H, 2 × CH) ppm. ^{13}C NMR (500 MHz, [D$_6$]DMSO): δ = 21.3, 24.4,

31.3 (CH_2), 54.1 (CH) 153.6 (CNR), 214.2 (CO), 219.6 (CO) ppm. Single crystals suitable for X-ray diffraction analysis were obtained by layering hexane on top of a DCM solution of the compound.

***fac-cis*-[Mn(CO)$_3$(smb)$_2$Br] (12):** Yield 72 mg, 52.5 μmol, 75%. IR: $\tilde{\nu}$ = 2177 (νCN stretching), 2035, 1982, 1937 (νCO stretching) cm^{-1}. ESI-MS (MeOH): *m*/*z* (%) = 504.0 (20) $[M]^+$. $C_{21}H_{18}BrMnN_2O_3$ (481.23): calcd. C 52.41, H 3.78, N 5.82; found C 53.02, H 3.94, N 5.62. ^{1}H NMR (360 MHz, [D$_6$]DMSO): δ = 1.60–1.69 (m, *J* = 5.8 Hz, 6 H, 2 × CH_3), 5.53–5.58 (m, *J* = 5.5 Hz, 2 H, 2 × CH), 7.36–7.50 (m, *J* = 5.2 Hz, 10 H, 10 × benzyl-CH) ppm. ^{13}C NMR (500 MHz, [D$_6$]DMSO): δ = 24.5 (CH_3), 55.0 (CN-CH), 56.0 (CN-CH), 125.3 (benzyl-CH), 128.4 (benzyl-CH), 129.0 (benzyl-CH), 138.6 (benzyl-CH), 155.6 (CNR), 214.0 (CO), 219.2 (CO) ppm.

***fac-cis*-[Mn(CO)$_3$(tmb)$_2$Br] (13):** Yield 86 mg, 174 μmol, 87%. IR: $\tilde{\nu}$ = 2172 (νCN stretching), 2031, 1977, 1931 (νCO stretching) cm^{-1}. ESI-MS (MeOH): *m*/*z* (%) = 528.2 (20) $[M]^+$. $C_{21}H_{34}BrMnN_2O_3$ (497.35): calcd. C 50.71, H 6.90, N 5.63; found C 49.83, H 6.53, N 5.39. ^{1}H NMR (360 MHz, [D$_6$]DMSO): δ = 1.08 (s, 18 H, 6 × C4-CH_3), 1.45 (s, 12 H, 4 × C2-CH_3), 1.70 (s, 4 ×, 2 × CH_2) ppm. ^{13}C NMR (500 MHz, [D$_6$]DMSO): δ = 30.6 (CH_3), 30.7 (CH_3), 30.8 (CH_3), 31.4 (CH_3), 31.21, 52.6, 60.5 (CH_2), 153.8 (CNR), 214.2 (CO), 219.6 (CO) ppm.

***fac-cis*-[Mn(CO)$_3$(mibi)$_2$Br] (14):** Yield 36 mg, 80 μmol, 40%. IR: $\tilde{\nu}$ = 2191 (νCN stretching), 2035, 1982, 1937 (νCO stretching) cm^{-1}. ESI-MS (MeOH): *m*/*z* (%) = 365.1 (100) $[M]^+$. $C_{15}H_{22}BrMnN_2O_5$ (445.19): calcd. C 40.47, H 4.99, N 6.29; found C 40.25, H 4.88, N 6.30. ^{1}H NMR (360 MHz, [D$_6$]DMSO): δ = 1.10 (s, 12 H, 4 × C1-CH_3), 3.50 (s, 6 H, 2 × OCH_3), 3.83 (s, 4 H, 2 × CH_2) ppm. ^{13}C NMR (500 MHz, [D$_6$]DMSO): δ = 22.05 (CH_3), 22.09 (CH_3), 49.4 (CH_2), 52.0 (CH_2), 73.5 (OCH_3), 154.4 (CNR), 213.9 (CO), 219.3 (CO) ppm. Single crystals suitable for X-ray diffraction analysis were obtained by layering hexane on top of a DCM solution of the compound.

Detection of CO Release through the Myoglobin Assay: An aliquot (150 μL) of a 700 μM solution of horse heart myoglobin (Mb) was placed in a phosphate buffer solution (2850 μL, pH 7.4) to give a final Mb concentration of 35 μM. Sodium dithionite was added to the solution until the complete reduction of Fe was observed spectroscopically. Finally, the selected complex dissolved in DCM was added (maximum amount of DCM < 5%) to give a final concentration of 35 μM. A follow-up UV/Vis spectroscopic analysis was performed to monitor the Q band as an indication of the possible binding of CO, as described previously.[37] The Mn-based CORMs (i.e., **9**–**14**) were irradiated with a UV lamp for 5 min between each UV/Vis trace. The Re-based CORMs (i.e., **3**–**8**) were not irradiated, and the spectroscopic changes of the Q band were monitored as a function of time.

Antibacterial Tests: An aliquot (10 μL) of a 50 mg/mL solution of the selected complex in 1–5% DMSO was dropped on an agar solution in Petri dishes inoculated by a single colony of *E. coli* immediately before. The incubation was performed at 37 °C for 24 h. For the MIC determination, serial dilutions were prepared in 1–5% DMSO. This solution (500 μL) was injected into lysogeny broth (LB) medium (5 mL) immediately after inoculation by a single colony of *E. coli* (the final concentrations of the complexes were 1024 to 0.0625 μg/mL). Incubation was performed at 37 °C for 24 h. This method is similar to a procedure described previously.[68]

Fibroblasts Proliferation Assay: After 26 passages, 3T3 mice fibroblasts cells were cultured in Dulbecco's modified Eagle's medium (DMEM) supplemented with 25 mM glucose, 1 mM sodium pyruvate, 10% fetal bovine serum (FBS), and 1% penicillin/streptomycin at pH 7.4. The assay was performed in 96-well plates with ca. 1000 cells per well proliferated at 37 °C in the presence of 95% air and 5% CO_2. After 1 d, the twelve compounds were added to the cells under a dim light to give a final concentration of 20 or 100 μM. After the administration of the compounds, half of the cultures were exposed to light (neon lamp at a distance of 60 cm) for 30 min, and the other half were kept in darkness. All of the cultures were subsequently kept in the dark for the rest of the incubation time. After 1, 2, and 3 d, a 3-(4,5-dimethylthiazol-2-yl)-2,5-diphenyltetrazolium bromide (MTT) cell proliferation assay was performed as follows: the yellow MTT was added to the cells to give a final concentration of 4 mM, and the cultures were incubated in the dark at 37 °C for 4 h. The medium was then removed, and DMSO (100 μL) was added to each well. After 30 min of incubation at room temperature in the dark, the optical density at λ = 550 nm was read with a plate reader.[69]

Acknowledgments

Financial support from the Swiss National Science Foundation (grant number PP00P2_144700) is gratefully acknowledged.

[1] A. Pamplona, A. Ferreira, J. Balla, V. Jeney, G. Balla, S. Epiphanio, Â. Chora, C. D. Rodrigues, I. P. Gregoire, M. Cunha-Rodrigues, *Nat. Med.* **2007**, *13*, 703–710.
[2] M. Ferrándiz, N. Maicas, I. Garcia-Arnandis, M. Terencio, R. Motterlini, I. Devesa, W. van den Berg, M. Alcaraz, *Ann. Rheum. Dis.* **2008**, *67*, 1211–1217.
[3] Â. A. Chora, P. Fontoura, A. Cunha, T. F. Pais, S. Cardoso, P. P. Ho, L. Y. Lee, R. A. Sobel, L. Steinman, M. P. Soares, *J. Clin. Invest.* **2007**, *117*, 438.
[4] J. D. Beckman, J. D. Belcher, J. V. Vineyard, C. Chen, J. Nguyen, M. O. Nwaneri, M. G. O'Sullivan, E. Gulbahce, R. P. Hebbel, G. M. Vercellotti, *Am. J. Physiol.-Heart C* **2009**, *297*, H1243–H1253.
[5] S. K. Bains, R. Foresti, J. Howard, S. Atwal, C. J. Green, R. Motterlini, *Arterioscler. Thromb. Vasc. Biol.* **2010**, *30*, 305–312.
[6] A. Nicolai, M. Li, D. H. Kim, S. J. Peterson, L. Vanella, V. Positano, A. Gastaldelli, R. Rezzani, L. F. Rodella, G. Drummond, *J. Hypertens.* **2009**, *53*, 508–515.
[7] M. Di Pascoli, L. Rodella, D. Sacerdoti, M. Bolognesi, S. Turkseven, N. G. Abraham, *Biochem. Biophys. Res. Commun.* **2006**, *340*, 935–943.
[8] B. S. Zuckerbraun, T. R. Billiar, S. L. Otterbein, P. K. Kim, F. Liu, A. M. Choi, F. H. Bach, L. E. Otterbein, *J. Exp. Med.* **2003**, *198*, 1707–1716.
[9] G. Sass, M. C. P. Soares, K. Yamashita, S. Seyfried, W. H. Zimmermann, T. Eschenhagen, E. Kaczmarek, T. Ritter, H. D. Volk, G. Tiegs, *J. Hepatol.* **2003**, *38*, 909–918.
[10] R. Motterlini, P. Sawle, J. Hammad, B. E. Mann, T. R. Johnson, C. J. Green, R. Foresti, *Pharmacol. Res.* **2013**, *68*, 108–117.
[11] L. E. Otterbein, *Resp. Care* **2009**, *54*, 925–932.
[12] S. T. Omaye, *Toxicology* **2002**, *180*, 139–150.
[13] F. Zobi, *Future Med. Chem.* **2013**, *5*, 175–188.
[14] S. García-Gallego, G. J. Bernardes, *Angew. Chem. Int. Ed.* **2014**, *53*, 9712–9721.
[15] S. H. Heinemann, T. Hoshi, M. Westerhausen, A. Schiller, *Chem. Commun.* **2014**, *50*, 3644–3660.
[16] U. Schatzschneider, *Br. J. Pharmacol.* **2015**, *172*, 1638–1650.
[17] C. C. Romao, W. A. Blättler, J. D. Seixas, G. J. Bernardes, *Chem. Soc. Rev.* **2012**, *41*, 3571–3583.
[18] S. J. Carrington, I. Chakraborty, P. K. Mascharak, *Chem. Commun.* **2013**, *49*, 11254–11256.
[19] I. Chakraborty, S. J. Carrington, P. K. Mascharak, *Acc. Chem. Res.* **2014**, *47*, 2603–2611.

[20] M. A. Gonzalez, M. A. Yim, S. Cheng, A. Moyes, A. J. Hobbs, P. K. Mascharak, *Inorg. Chem.* **2011**, *51*, 601–608.
[21] U. Schatzschneider, *Inorg. Chim. Acta* **2011**, *374*, 19–23.
[22] R. Motterlini, J. E. Clark, R. Foresti, P. Sarathchandra, B. E. Mann, C. J. Green, *Circ. Res.* **2002**, *90*, e17–e24.
[23] P. Engelking, W. Lineberger, *J. Am. Chem. Soc.* **1979**, *101*, 5569–5573.
[24] G. Dördelmann, T. Meinhardt, T. Sowik, A. Krueger, U. Schatzschneider, *Chem. Commun.* **2012**, *48*, 11528–11530.
[25] G. Dördelmann, H. Pfeiffer, A. Birkner, U. Schatzschneider, *Inorg. Chem.* **2011**, *50*, 4362–4367.
[26] H. Pfeiffer, A. Rojas, J. Niesel, U. Schatzschneider, *Dalton Trans.* **2009**, 4292–4298.
[27] J. Niesel, A. Pinto, H. W. Peindy N'Dongo, K. Merz, I. Ott, R. Gust, U. Schatzschneider, *Chem. Commun.* **2008**, 1798–1800.
[28] I. Chakraborty, S. Sengupta, S. Das, S. Banerjee, A. Chakravorty, *Dalton Trans.* **2003**, 134–140.
[29] S. Sengupta, I. Chakraborty, A. Chakravorty, *Eur. J. Inorg. Chem.* **2003**, 1157–1160.
[30] G. E. Mullen, P. J. Blower, D. J. Price, A. K. Powell, M. J. Howard, M. J. Went, *Inorg. Chem.* **2000**, *39*, 4093–4098.
[31] S. O. Matondo, P. Mountford, D. J. Watkin, W. B. Jones, S. R. Cooper, *J. Chem. Soc., Chem. Commun.* **1995**, 161–162.
[32] M. Stebler, A. Gutierrez, A. Ludi, H. B. Buergi, *Inorg. Chem.* **1987**, *26*, 1449–1451.
[33] T. Al Salih, M. T. Duarte, J. J. F. da Silva, A. M. Galvão, M. F. C. G. da Silva, P. B. Hitchcock, D. L. Hughes, C. J. Pickett, A. J. Pombeiro, R. L. Richards, *J. Chem. Soc., Dalton Trans.* **1993**, 3015–3023.
[34] F. Zobi, O. Blacque, R. A. Jacobs, M. C. Schaub, A. Y. Bogdanova, *Dalton Trans.* **2012**, *41*, 370–378.
[35] F. Zobi, O. Blacque, *Dalton Trans.* **2011**, *40*, 4994–5001.
[36] F. Zobi, L. Kromer, B. Spingler, R. Alberto, *Inorg. Chem.* **2009**, *48*, 8965–8970.
[37] F. Zobi, A. Degonda, M. C. Schaub, A. Y. Bogdanova, *Inorg. Chem.* **2010**, *49*, 7313–7322.
[38] F. Zobi, A. Degonda, *Nucl. Med. Biol.* **2010**, *37*, 712.
[39] M. Patra, M. Wenzel, P. Prochnow, V. Pierroz, G. Gasser, J. E. Bandow, N. Metzler-Nolte, *Chem. Sci.* **2015**, *6*, 214–224.
[40] U. Schatzschneider, *Inorg. Chim. Acta* **2011**, *374*, 19–23.
[41] R. D. Rimmer, A. E. Pierri, P. C. Ford, *Coord. Chem. Rev.* **2012**, *256*, 1509–1519.
[42] H.-M. Berends, P. Kurz, *Inorg. Chim. Acta* **2012**, *380*, 141–147.
[43] P. Govender, S. Pai, U. Schatzschneider, G. S. Smith, *Inorg. Chem.* **2013**, *52*, 5470–5478.
[44] D. Moka, F. Baer, P. Theissen, C. Schneider, M. Dietlein, E. Erdmann, H. Schicha, *Eur. J. Nucl. Med.* **2001**, *28*, 602–607.
[45] A. L. Baggish, C. A. Boucher, *Circulation* **2008**, *118*, 1668–1674.
[46] C. C. Ko, L. T. L. Lo, C. O. Ng, S. M. Yiu, *Chem. Eur. J.* **2010**, *16*, 13773–13782.
[47] P. Treichel, G. Dirreen, H. Mueh, *J. Organomet. Chem.* **1972**, *44*, 339–352.
[48] P. Treichel, D. W. Firsich, G. Essenmacher, *Inorg. Chem.* **1979**, *18*, 2405–2409.
[49] M. G. Drew, B. J. Brisdon, A. M. Watts, *Polyhedron* **1984**, *3*, 1059–1063.
[50] F. Zobi, B. Spingler, R. Alberto, *Dalton Trans.* **2008**, 5287–5289.
[51] F. Zobi, O. Blacque, G. Steyl, B. Spingler, R. Alberto, *Inorg. Chem.* **2009**, *48*, 4963–4970.
[52] P. Morel, P. Schaffer, J. F. Valliant, *J. Organomet. Chem.* **2003**, *668*, 25–30.
[53] M. A. Stewart, C. E. Moore, T. B. Ditri, L. A. Labios, A. L. Rheingold, J. S. Figueroa, *Chem. Commun.* **2011**, *47*, 406–408.
[54] B. J. Coe, S. J. Glenwright, *Coord. Chem. Rev.* **2000**, *203*, 5–80.
[55] L. K. Wareham, R. K. Poole, M. Tinajero-Trejo, *J. Biol. Chem.* **2015**, *290*, 18999–19007.
[56] J. S. Ward, J. M. Lynam, J. Moir, I. J. Fairlamb, *Chem. Eur. J.* **2014**, *20*, 15061–15068.
[57] C. Nagel, S. McLean, R. K. Poole, H. Braunschweig, T. Kramer, U. Schatzschneider, *Dalton Trans.* **2014**, *43*, 9986–9997.
[58] A. L. Barry, *The Antimicrobic Susceptibility Test: Principles and Practices*, Lippincott Williams & Wilkins, Philadelphia, **1976**.
[59] A. P. MacGowan, R. Wise, *J. Antimicrob. Chemother.* **2001**, *48*, 17–28.
[60] J. t. Cosier, A. Glazer, *J. Appl. Crystallogr.* **1986**, *19*, 105–107.
[61] E. Blanc, D. Schwarzenbach, H. Flack, *J. Appl. Crystallogr.* **1991**, *24*, 1035–1041.
[62] G. M. Sheldrick, *Acta Crystallogr., Sect. C* **2015**, *71*, 3–8.
[63] N. Rega, S. S. Iyengar, G. A. Voth, H. B. Schlegel, T. Vreven, M. J. Frisch, *J. Phys. Chem. B* **2004**, *108*, 4210–4220.
[64] A. D. Becke, *J. Chem. Phys.* **1993**, *98*, 5648–5652.
[65] P. J. Hay, W. R. Wadt, *J. Chem. Phys.* **1985**, *82*, 299–310.
[66] P. J. Hay, W. R. Wadt, *J. Chem. Phys.* **1985**, *82*, 270–283.
[67] W. R. Wadt, P. J. Hay, *J. Chem. Phys.* **1985**, *82*, 284–298.
[68] R. Jones, A. Barry, T. Gavan, J. Washington (Eds.), *Manual of Clinical Microbiology*, 4th ed., American Society for Microbiology, Washington, DC, **1985**, 972–977.
[69] P. Twentyman, M. Luscombe, *Brit. J. Cancer* **1987**, *56*, 279